



## Article

# The Influence of Burn Severity on Post-Fire Spectral Recovery of Three Fires in the Southern Rocky Mountains

Jaclyn Guz \*, Florencia Sangermano and Dominik Kulakowski

Graduate School of Geography, Clark University, 950 Main Street, Worcester, MA 01610, USA; fsangermano@clarku.edu (F.S.); dkulakowski@clarku.edu (D.K.)

\* Correspondence: jguz@clarku.edu or jaclynguz@gmail.com

**Abstract:** Increased wildfire activity and altered post-fire climate in the Southern Rocky Mountains has the potential to influence forest resilience. The Southern Rocky Mountains are a leading edge of climate change and have experienced record-breaking fires in recent years. The change in post-fire regeneration and forest resilience could potentially include future ecological trajectories. In this paper, we examined patterns of post-fire spectral recovery using Landsat time series. Additionally, we utilized random forest models to analyze the impact of climate and burn severity on three fire events in the Southern Rocky Mountains. Fifteen years following the fires, none of the burned stands fully recovered to their pre-fire spectral states. The results suggested that burn severity significantly impacted post-fire spectral recovery, but that influence may decrease as time since fire increases. The biggest difference in forest recovery was among fire events, indicating that post-fire climate may be influential in post-fire recovery. The mean and minimum growing-season temperatures were more significant to post-fire recovery than the variability in precipitation, which is consistent with field-based analysis. The present study indicated that, as warming continues, there may be changes in forest density where forests are not regenerating to their pre-fire spectral states. Additionally, this study emphasizes how high-elevation forests continue to regenerate after fires, but that regeneration is markedly affected by post-fire climate.

**Keywords:** forest resilience; fires; the Southern Rocky Mountains; climate change; Landsat; lodgepole pine; disturbances; regeneration



**Citation:** Guz, J.; Sangermano, F.; Kulakowski, D. The Influence of Burn Severity on Post-Fire Spectral Recovery of Three Fires in the Southern Rocky Mountains. *Remote Sens.* **2022**, *14*, 1363. <https://doi.org/10.3390/rs14061363>

Academic Editors: Lei Fan, Xiuzhi Chen, Frédéric Frappart, Yongxian Su and Yuanwei Qin

Received: 1 December 2021

Accepted: 9 February 2022

Published: 11 March 2022

**Publisher's Note:** MDPI stays neutral with regard to jurisdictional claims in published maps and institutional affiliations.



**Copyright:** © 2022 by the authors. Licensee MDPI, Basel, Switzerland. This article is an open access article distributed under the terms and conditions of the Creative Commons Attribution (CC BY) license (<https://creativecommons.org/licenses/by/4.0/>).

## 1. Introduction

### 1.1. Wildfires and Climate Change

Wildfires are burning in the Southern Rocky Mountains (e.g., Northern Colorado and Southern Wyoming), 22% more than any other time in the past 2000 years [1]. The previous record was established ~1100 years ago, during the Medieval Climate Anomaly (MCA). During the MCA, the Northern Hemisphere was 0.3 °C (0.5 °F) warmer than the 20th-century average and subalpine forests, ranging from 9000 to 10,000 ft, burned on average every 150 years. In contrast, over the past 2000 years, subalpine fires in the Southern Rocky Mountains burned a given spot on average every 230 years. In 2020, the Northern Hemisphere was 1.28 °C (2.3 °F) above the 20th-century average, and fires are now expected to occur, on average, every 117 years. This dramatic increase in the wildfire activity is directly related to the warmer–drier weather caused by climate change [1].

The 2020 fire season included three of the largest wildfires in Colorado's history and set records across the Western United States. Many fires in 2020 occurred in subalpine forests dominated by lodgepole pine (*Pinus contorta* var. *latifolia*). Subalpine forests were historically less impacted by fire suppression and other land management compared to lower elevation forests, making them good historians of climate–fire relationships [2]. Increased burning and hotter and drier post-fire climate conditions have consequences for tree regeneration, ecosystem connectivity, and total forested areas [1]. During the

MCA, increased fire activity and temperature converted the lower tree line from a dense closed-canopy forest to the lower-density ribbon forest we have today [3]. Additionally, burning during the MCA reduced ecosystem connectivity, which could negatively impact ecosystem conservation if it were to recur [2,4].

Lodgepole pine is a shade-intolerant, early successional species that regenerates rapidly after wildfires; its serotinous cones release seeds only when heated, giving the tree a post-fire advantage over other species. However, the number of serotinous cones produced by an individual tree or stand varies greatly and appears to be linked to disturbance regimes (especially fire frequency and severity) [5]. Although lodgepole pine has been thought to reproduce well under adverse conditions (e.g., following severe fires and altered post-fire climate) [5], recent evidence suggests that regeneration success is also affected by post-fire climate conditions (e.g., increased temperatures) in a manner that increases forest patchiness [6]. Additional research on non-serotinous Sierra lodgepole pine (*Pinus contorta* var. *murrayana*) suggested that regeneration is influenced by burn severity. A repeated high-severity fire can result in a lower tree seeding density compared with a low-severity fire followed by a high-severity fire, because a past high-severity fire may reduce the seedbank and other seed sources [7,8]. As wildfire frequency and severity increase, understanding the dynamic relationship among climate, vegetation, and fire regimes is evermore necessary for understanding post-fire regeneration and anticipating future forest dynamics.

### 1.2. Remote Sensing, Burn Severity, and Post-Fire Regeneration

Remotely sensed (RS) data are used in fire science to monitor the size and frequency of wildfires [9–11]. Additionally, space-borne sensors can be utilized in assessing climate and environmental conditions before and after fire events [12,13]. RS data also have been used for fire detection [14], assessing active fire behavior [15], characterizing burn severity [16], examining post-fire vegetation response [17–19] and identifying areas where vegetation recovery has been limited [20].

Fire severity describes the magnitude with which fire has affected the ecosystem. In general, fire severity is defined as a spectrum based on the percentage of vegetation that is killed in a fire. On one side of the spectrum, a low-severity fire consumes understory vegetation and leaves most trees alive. On the other side of the spectrum, high-severity fires are synonymous with crown fires that kill most trees and other vegetation. Spectral indices (SIs) are among the most common remote sensing techniques in fire science due to their conceptual simplicity and computational efficiency. The normalized burn ratio (NBR) has emerged as one of the most widely used SIs to track post-disturbance regeneration [21–23]. The NBR utilizes a ratio between the near-infrared (NIR) and short-wave infrared (SWIR) regions. Healthy, unburned vegetation is highly reflective in the NIR region and has a low reflectance in the SWIR portion of the electromagnetic spectrum. The SWIR region is strongly absorbed by the water content in vegetation or soil [24]. After a fire, burned areas have a low reflectance in the NIR region and a high reflectance in the SWIR region, which decreases the NBR [24,25]. The Monitoring Trends in Burn Severity (MTBS) program was established in 2006 to remotely map the extent, burned area, and burn severity of fires over 405 hectares in Western United States, Alaska, and Hawaii and fires over 202 hectares in Eastern United States and Puerto Rico using Landsat imagery for all fires since 1984 [26]. The MTBS program defined burn severity as a visible alteration of vegetation, dead biomass, and soil within a fire perimeter [26]. Low severity corresponds to damaged ground herbaceous vegetation, moderate severity correlates with mostly burned understory vegetation with some canopy mortality, and high severity indicates completely burned understory vegetation with major canopy mortality. These changes can be assessed tracking changes in SI estimates of burn severity. The differenced normalized burn ratio (dNBR) assesses the changes in the reflection of NIR and SWIR regions of vegetated surfaces resulting from fire [24]. The dNBR metric measures the difference between a pre- and post-fire NBR image, with typical values ranging between –2000 and 2000.

The MTBS program classified dNBR values into thematic classes to interpret the burn severity. A higher value of the dNBR indicates more severe damage (Table 1).

**Table 1.** Burn severity levels obtained calculating the differenced normalized burn ratio (dNBR), proposed by the United States Geological Survey.

Severity Level	dNBR Range (Scaled by 10 <sup>3</sup> )	Relationship to Ecological Damage
low severity	+100 to 269	damaged ground herbaceous vegetation
moderate severity	+270 to +659	completely burned understory vegetation with some canopy mortality
high severity	+660 to +1300	completely burned understory vegetation with major canopy mortality

### 1.3. Remote Sensing to Quantify Forest Resilience

In remote sensing applications, resilience or “recovery” is typically defined as a return or near-return to pre-fire spectral values [27]. However, it is important to note that a return to pre-fire spectral values may not always indicate a recovery of forest function, structure [28,29], or the same forest type [30]. Thus, using remote sensing to map post-fire regeneration trajectories focuses on a return to a pre-fire spectral reflectance in the growing season [29–31]. This paper defines forest resilience as the degree of perturbation (e.g., low, medium, and high fire severity levels) which a forest can absorb and return to a similar pre-spectral state [32,33].

In the present study, we examined patterns of post-fire spectral recovery following three fires in the Southern Rocky Mountains. Based on field validation in [6] these fires were of high severity and occurred in pure lodgepole pine (*Pinus contorta* var. *latifolia*) stands. Post-fire regeneration trajectories have been attributed to pre-fire conditions [30,34], burn severity [7], topography including slope, aspect, and elevation [35,36], and post-fire climate, including temperature and moisture [6]. Our primary objectives were as following: (1) to monitor forest resilience and quantify post-fire spectral change in the Southern Rocky Mountains following the fires; (2) to analyze how climate anomalies may have affected the rate of the post-fire spectral change; and (3) to analyze how the magnitude and rate of the post-fire spectral change are influenced by burn severity, topography, and geology. We broke down our analysis into three phases. In the first phase, we created a Landsat time series (LTS) using Google Earth Engine (GEE)’s Landsat-based Detection of Trends in Disturbance and Recovery (LandTrendr). We utilized the NBR to evaluate the presence of healthy and burned vegetation in the time series. The NBR time series was stratified by burn severity and allowed us to understand how burn severity impacted forest resilience (e.g., the degree of perturbation a forest can absorb and return to a similar pre-spectral state). In the second phase, we looked at understanding how the climate influenced the rate and magnitude of the post-fire recovery. In the third phase, we utilized random forests (RFs) to understand how topography, burn severity, fire regimes, and geological data interacted and influenced the rate and magnitude of the post-fire recovery. Given the likely importance of the climate and the topography on the post-fire recovery, we hypothesized the following: (1) the recovery to a pre-fire spectral state would vary by burn severity and elevation; and (2) the post-fire recovery would be influenced by growing-season climate conditions.

## 2. Materials and Methods

### 2.1. Study Area

We studied three wildfires that occurred in the Southern Rocky Mountains (extending from Northern New Mexico to Southern Wyoming) from 1999 to 2006 (Figure 1, Table 2) in forests dominated by lodgepole pine [6]. For the past seven decades, the Southern Rocky Mountains have felt the effects of warmer and drier conditions resulting from the climate change in North America [6]. Ecological disturbances (e.g., windstorms, insect outbreaks, and wildfires) have increased primarily because of climate change. Increased disturbances have been especially prominent in forests dominated by lodgepole pine.



Furthermore, the climate change in the Southern Rocky Mountains has the potential to influence forest resilience and ecological trajectories. Disturbances have been pronounced in forests dominated by lodgepole pine [6].

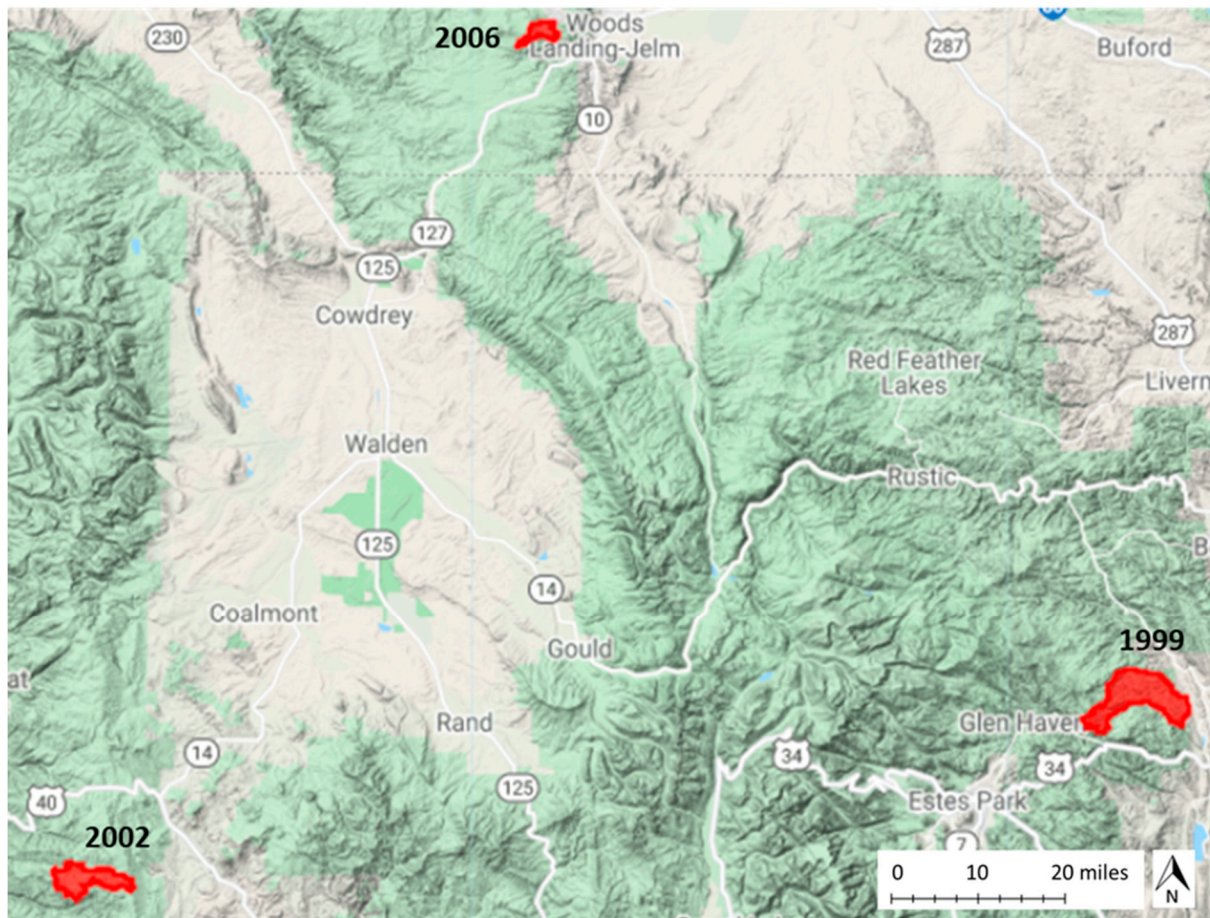


**Figure 1.** Map of the study area.

**Table 2.** Site and stand characteristics of burned forest stands.

Fire Year	1999	2002	2006
size (ha)	10.600	4397	1200
mean elevation (masl)	2426	2825	2645
dominant aspect	ESE	SE	E

Refer to [6] for more detailed information about field validations of fires and post-fire regeneration [6].

## 2.2. Data Analysis

### 2.2.1. Landsat Data Pre-Processing and Segmentation

We used GEE's implementation of the LandTrendr temporal segmentation algorithm to derive the yearly LTS maps of the post-fire recovery. LandTrendr incorporates temporal segmentation and a fitting approach for each pixel of the LTS. LandTrendr identifies breakpoints (vertices) and determines straight-line trajectories that result in a fitted-to-vertex (FTV) time series. With the FTV time series, LandTrendr provides information on the magnitude and rate of post-fire recovery.

In this study, we used the United States Geological Survey (USGS) Landsat Surface Reflectance Tier 1 data from Landsat 5, 7, and 8 to examine spectral recovery trajectories following fires in 1999, 2002, and 2006. Clouds and cloud shadows were filtered using masks produced by the CFMask algorithm and included five-year pre-fire to 15-year post-fire time series, including all images from 1st June to 30th September for each year. LandTrendr

utilized medoid compositing, a multi-dimensional analog of the median, to aggregate all the images in the LTS. For each pixel, the medoid was selected from the available data, with the result that a single observation for each pixel preserved the relationship between Landsat bands. This output was a new annual LTS where the pixel values between vertices were interpolated and reduced the year-to-year noise. The result was an LTS with a single summer observation per year for a 20-year time series.

### 2.2.2. Phase 1: Monitoring Forest Resilience

We were interested in understanding how burn severity influences forest resilience. To answer this question, we extracted thematic burn severity categories (i.e., low, moderate, and high) from the MTBS program for each fire and created an LTS for the fire segregated by burn severity. This resulted in three LTSs per fire stratified by burn severity (low-, moderate-, and high-severity LTSs) for all pixels. These time series were made using the entire population of pixels in each burn severity group. The mean NBRs were extracted five-, 10-, and 15-year post-fire.

We then calculated the “annual %NBR recovery”, defined as the magnitude of the NBR recovery divided by the magnitude of the fire-induced decrease in the NBR multiplied by 100 (Figure 2). The “annual %NBR recovery” time series allowed us to calculate how an area recovered annually in relation to its pre-fire spectral state as a measure of forest recovery.

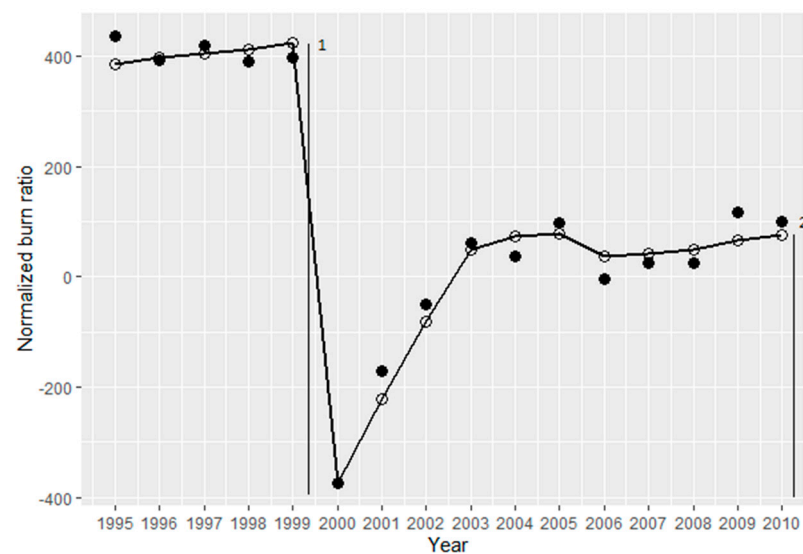


**Figure 2.** A conceptual example of Landsat-based Detection of Trends in Disturbance and Recovery (LandTrendr) fitting the normalized burn ratio (NBR) values to the spectral-temporal segments of a pixel burned at a high severity level in the 1999 Fire. The original NBRs are displayed by black circles, and the fitted are displayed by open circles. The percent of the NBR change in 2010 was defined as distance 2 divided by distance 1 multiplied by 100.

### 2.2.3. Phase 2: Climate Influence on Resilience

Using the Parameter-elevation Regressions on Independent Slopes Model (PRISM) data, we assessed differences in the summer (June–September) and winter (October–March) precipitations and temperatures 15-year post-fire and analyzed the effects of cumulative climate anomalies on the annual NBR recovery. The post-fire cumulative climate anomalies considered were changes in the minimum post-fire winter and summer temperatures, average temperatures, maximum temperatures, total precipitations, and average precipitations. All variables were calculated as site-specific cumulative climate anomalies. We utilized cumulative climate anomalies, because vegetation responds to the accumulated effects of climate change during regeneration. This decision allowed us to account for interannual climate variations of the growing and winter seasons. Cumulative climate anomalies provide a broader perspective on the deficit or surplus of the precipitation and the temperature. We

defined the reference conditions for the precipitation and the temperature over the 30 years from 1990 to 2020.

Backward stepwise selection models were utilized to examine the effect of cumulative climate anomalies on post-fire recovery. The models were run based on the fire event, fire severity, and season (summer vs. winter) for a total of 18 backward stepwise selection models. Post-fire cumulative climate anomalies were used to model the influence of the NBR for the 15-year post-fire period. A 15-year post-fire period was chosen, because lodgepole pine requires 5–15 years to reach maturity and produce serotinous seeds [37]. Data were analyzed using R statistical package [38,39]. Other packages included “*tidyverse*”, “*caret*”, and “*leaps*”. The *stepAIC()* function chooses the best model, and the *leaps* package provides the tuning parameter “*nvmax*” that allows specifying the maximal number of predictors to incorporate in the model. The mean absolute error (MAE) statistical metric was used to compare the models and automatically choose the best one, where the best is defined as the model that minimizes the MAE.

#### 2.2.4. Phase 3: Influence of the Topography, Burn Severity, Fire Regimes, and Geological Data on Resilience

Shuttle Radar Topography Mission (SRTM) digital elevation data, LANDFIRE Fire Regime Groups (FRG) v1.2.0 dataset, and PRISM Monthly Spatial Climate Dataset data were obtained from the GEE platform. The SRTM elevation data were used to extract the slope, elevation, and aspect for each fire. LANDFIRE FRG provided the mean fire return interval, which quantified the average period between fires under the presumed historical fire regime. Time-varying variables, specific to each year and site, included the post-fire climate derived from PRISM Monthly Spatial Climate Dataset data. The ESRI Living Atlas provided the Soil Survey Geographic Database (SSURGO) that includes Ecological Section (soils and landcover), USA Hydraulic Group, USA Soils Bedrock Depth, USA Soils Hydric Class, and USA Soils Drainage Class (Table 3).

We developed regression tree models using random forests (RFs) [40] to examine the variability in post-fire recovery for 15 years in relation to topography, soil variables, and burn severity (low, moderate, and high) in R [38,41]. We took the LandTrendr time series bands and extracted the magnitude and rate of spectral recovery for the 15-year post-fire period. We developed regression tree models of the following: (1) the magnitude of spectral recovery; and (2) the rate of recovery. The RF is an extension of classification and regression trees analysis, whereby trees are constructed by repeatedly dividing the data into two mutually exclusive groups [40]. We chose the RF as a means for determining important predictors of lodgepole pine regeneration, because it is known to work well with complex ecological data [42]. We generated node purities, analogous to Gini-based importance, to identify the most important variables in the prediction. The node purity was calculated based on the reduction in the sum of squared errors whenever a variable was chosen to split a tree.

Each model was generated by partitioning the dependent variable into 75% for the model training and 25% for the model testing. We then compared the predicted value with the actual value in the test data and analyzed the model’s accuracy. To test the accuracy of our model, we used the MAE. To improve the predictive power of our models, we tuned the parameters *ntrees* (the number of trees in the forest) and *maxnodes* (the maximum number of terminal nodes that trees in the forest can have). The best parameters were the ones with the lowest MAE.

**Table 3.** Explanatory topographic variables impact on the NBR change (%).

Variable Name	Data Type	Variable Definition	Significance for the NBR Recovery
Elevation	continuous	elevation on the latitude (m)	Reflecting the size and shape of stand-replacing fire Common in upper elevations
Aspect	discrete	direction the slope faces	North-facing slopes are cooler than south-facing slopes
Slope	continuous	Slope gradient (°)	Steeper slopes retain less moisture and may be less suitable for regeneration.
Fire Regime Group (FRG)	discrete	The LANDFIRE Fire dataset provides presumed historical fire regimes within landscapes based on interactions between vegetation dynamics, fire spread, fire effects, and spatial contexts.	Lodgepole pine is limited to crown fires every 200–350 years.
USA Soils Hydraulic Group	discrete	The hydrologic soil group is displayed in seven classes that describe the rate at which the soil absorbs rainfall.	The physical properties of soil affect the rate at which water is absorbed. Hydrologic soil groups provide the rate at which water infiltrates the soil.
USA Soils Bedrock Depth	discrete	The shallowest depth to bedrock from the top of the soil is displayed.	Bedrock is the material under soils.
USA Soils Hydric Class	discrete	Hydric soils for conditions of saturation, flooding, or ponding long enough during the growing season to develop anaerobic conditions for the under part of the soil are displayed.	Hydric soils drain poorly and may have additional moisture.
USA Soils Drainage Class	discrete	Soils are classified in seven classes based on the rate of water infiltration.	The rate at which water drains into the soil has a direct effect on how plants can grow.
Burn Severity	discrete	The Monitoring Trends in Burn Severity (MTBS) provided burn severity.	Lodgepole pine is adapted to high-severity fires. Mixed-severity and low-severity fires can impact forest recovery.

### 3. Results

#### 3.1. Assessing Forest Resilience

Post-fire NBR recovery varied non-linearly by fire severity, time since fire, and particular fire event (Figure 3). Fifteen years following fires, none of the burned stands fully recovered to their pre-fire NBR spectral states. However, the percent of the annual NBR recovery was greatest in patches burned at high severity levels (58% to 90%), in contrast to patches burned at moderate severity levels (50% to 82%) and low severity levels (46% to 62%) (Table 4). In low-severity areas, the vegetation changes following fires were most likely due to the greater opportunity for the establishment and growth of new species instead of regeneration. Post-fire %NBR recovery increased annually in areas burned at both medium and low severities (Table 4). This may be because the fire thinned out the stand and allowed other trees to grow more or because the fire was intense enough to release some seeds from serotinous cones. [6].

Only the stands that were burned in 2006 were able to recover to a near pre-fire spectral state, indicating the most resilience. The stands that were burned in 2002 and 1999 did not recover to a near pre-fire spectral state (Figure 3). When comparing the NBR spectral values 15 years post-fire, there was no difference in the NBR spectral values among fire severities in individual fire events, indicating that burn severity may not be the most important variable in determining resilience.



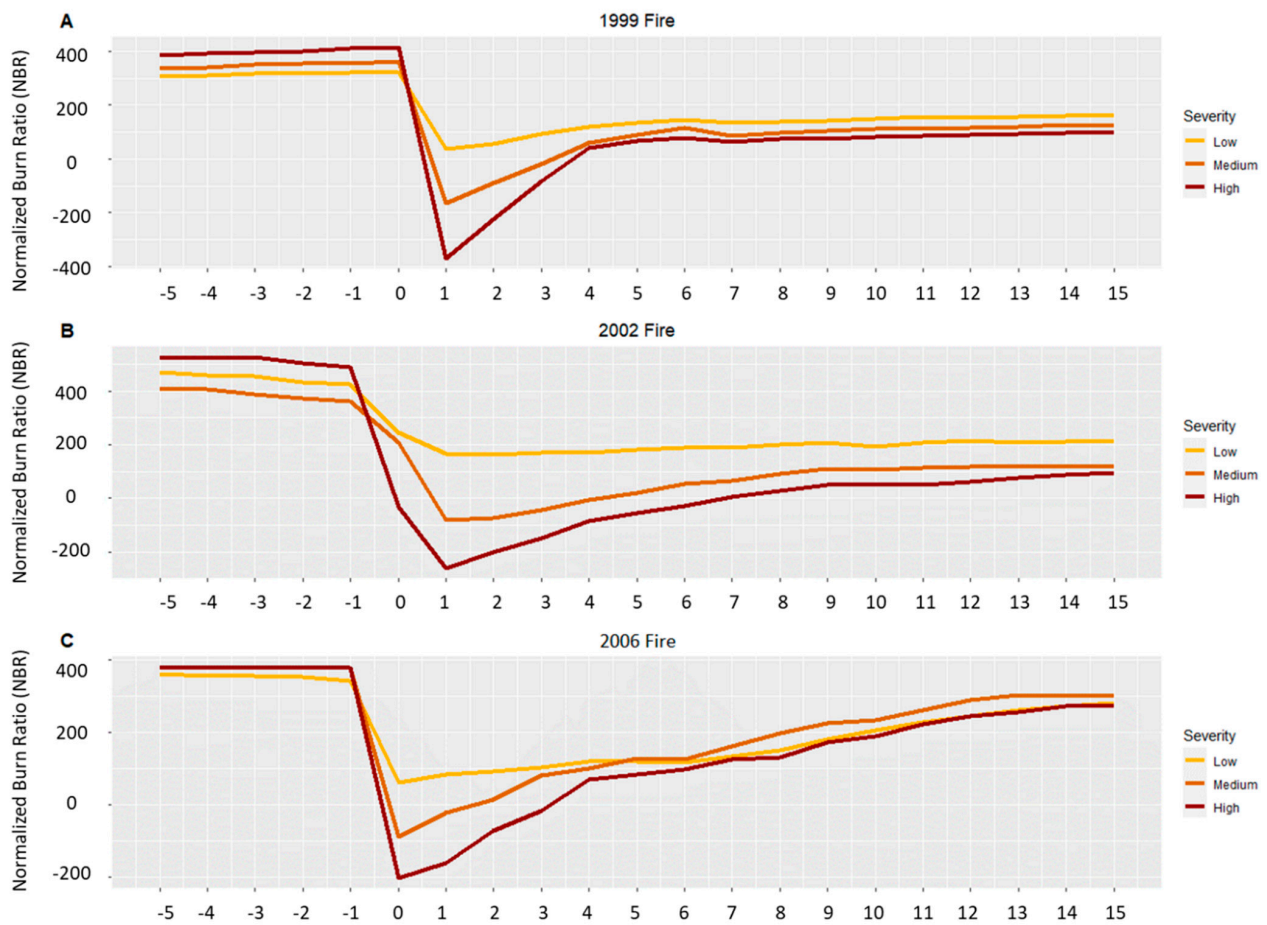


Figure 3. Post-fire %NBR recovery by burn severity.

Table 4. Post-fire %NBR recovery by burn severity.

Fire	Severity	Five Years Post-Fire	Ten Years Post-Fire	Fifteen Years Post-Fire
1999	high	56.10	55.31	59.99
1999	medium	51.60	54.59	58.17
1999	low	36.20	41.68	45.81
2002	high	82.50	67.06	58.10
2002	medium	17.49	40.72	50.40
2002	low	17.49	32.94	41.89
2006	high	62.90	68.79	89.97
2006	medium	41.48	66.84	81.61
2006	low	27.84	46.14	61.55

### 3.2. Climate Influence on the %NBR Recovery

The backward stepwise regression produced models showing that the minimum and mean temperatures of the summer season were highly influential in post-fire recovery. All insignificant variables were removed from the model, and significant variables were reported in Table 5. The tolerances were calculated for each model and the interaction between the temperature variables and the precipitation. However, when the interaction term was removed, the models were no longer significant. Therefore, these variables were included in the model, despite their collinearity. Overall, the change in the temperature (mean and minimum growing-season temperatures) was more significant for post-fire



recovery than the variability in precipitation (Table 5). The total annual precipitation was important only in the 1999 fire, where there was a small climate anomaly for the decreased precipitation. The minimum growing-season temperature was important for all the models, except for high-severity patches in the 1999 fire. The mean growing-season and winter temperatures were statistically important for all the 1999 fire models (Table 5), indicating that summer temperature may be an influential variable for post-fire recovery.

**Table 5.** Regression parameters from the backward stepwise regression conducted between the %NBR change and climate variables.

Fire	Severity	Season	Variable	Estimate	SE	t-Value	Pr (> t )	R <sup>2</sup>	p-Value
1999	high	summer season	intercept	28.63	10.94	2.62	0.05	0.33	0.09
			ppt	−0.02	0.01	−1.90	0.10		
1999	medium	summer season	intercept	58.36	22.22	2.62	0.03	0.50	0.11
			t <sub>mean</sub>	−1.60	1.57	−1.02	0.34		
			t <sub>min</sub>	1.66	0.90	1.84	0.11		
1999	low	summer season	intercept	44.69	14.73	3.04	0.02	0.61	0.05
			t <sub>mean</sub>	−1.42	1.04	1.04	0.22		
			t <sub>min</sub>	1.41	0.60	0.60	0.06		
1999	high	winter season	intercept	20.78	9.69	2.14	0.07	0.49	0.02
			ppt	−0.03	0.00	−2.97	0.02		
1999	medium	winter season	intercept	14.40	10.88	1.39	0.21	0.52	0.01
			ppt	−0.03	0.00	−3.12	0.02		
1999	low	winter season	intercept	7.71	7.76	0.90	0.40	0.53	0.04
			ppt	−0.16	0.00	−1.89	0.10		
			t <sub>mean</sub>	0.49	0.53	0.91	0.39		
2002	high	summer season	intercept	77.74	2.07	37.49	0.00	0.91	0.00
			t <sub>mean</sub>	−0.06	0.14	−0.43	0.68		
			t <sub>min</sub>	−0.66	0.07	−0.96	0.00		
2002	medium	summer season	intercept	25.20	3.76	6.70	0.00	0.87	0.00
			t <sub>mean</sub>	0.45	0.25	1.80	0.12		
			t <sub>min</sub>	0.95	0.13	7.16	0.00		
2002	low	summer season	intercept	22.26	2.07	10.73	0.00	0.91	0.00
			t <sub>mean</sub>	0.06	0.13	0.42	0.68		
			t <sub>min</sub>	0.65	0.07	8.95	0.00		
2002	high	winter season	intercept	76.32	1.95	39.03	0.00	0.87	0.00
			t <sub>max</sub>	0.44	0.06	6.58	0.00		
			t <sub>mean</sub>	−1.02	0.17	−5.95	0.00		
2002	medium	winter season	intercept	28.43	2.79	10.15	0.00	0.89	0.00
			t <sub>max</sub>	−0.60	0.09	−6.17	0.00		
			t <sub>mean</sub>	1.83	0.24	7.43	0.00		
2002	low	winter season	intercept	23.67	1.95	12.10	0.00	0.87	0.00
			t <sub>max</sub>	−0.44	0.06	−6.58	0.00		
			t <sub>mean</sub>	1.028	0.17	5.95	0.00		
2006	high	summer season	intercept	67.42	8.06	8.36	0.00	0.81	0.00
			t <sub>mean</sub>	−2.17	0.73	−2.96	0.02		
			t <sub>min</sub>	1.87	0.46	4.04	0.00		
2006	medium	summer season	intercept	65.27	9.88	6.60	0.00	0.84	0.00
			t <sub>max</sub>	−1.33	0.41	−3.21	0.01		
			t <sub>min</sub>	0.96	0.14	6.68	0.00		

Table 5. Cont.

Fire	Severity	Season	Variable	Estimate	SE	t-Value	Pr (> t )	R <sup>2</sup>	p-Value
2006	low	summer season	intercept	20.45	2.11	9.67	0.00	0.75	0.00
			t <sub>min</sub>	0.43	0.08	5.11	0.00		
2006	high	winter season	intercept	46.69	3.03	15.41	0.00	0.65	0.00
			t <sub>min</sub>	0.58	0.14	4.04	0.00		
2006	medium	winter season	intercept	37.55	3.72	10.09	0.00	0.65	0.00
			t <sub>min</sub>	0.72	0.17	4.02	0.00		
2006	low	winter season	intercept	22.12	1.60	13.77	0.00	0.83	0.00
			t <sub>min</sub>	0.49	0.07	6.35	0.00		

Note: The significance level was based on a 90% confidence level.

### 3.3. RF Analysis

In the RF analysis, burn severity was the most important variable that influenced post-fire spectral recovery (Table 6), indicating that burn severity plays a role in resilience. This can be explained by lodgepole pine's common prolific initial post-fire regeneration [6]. However, when comparing post-fire spectral values 15 years post-fire, there was not a significant impact, suggesting that fire severity may impact regeneration following high-severity fires, but the importance of fire severity on regeneration may decrease over the long term. An increase in the elevation correlated with an increase in the magnitude and rate of post-fire NBR recovery. Elevations of >2155 m had the highest magnitude and rate of recovery. Slopes of >28 degrees had decreased recovery. Northeast- and northwest-facing slopes had the greatest post-fire recovery. The higher spectral recovery indicated the greater regeneration of forest cover regeneration in high-severity and high-elevation burns. Soil and substrate compositions did not make a significant impact on post-fire spectral recovery trends.

Table 6. Random forest magnitude and rate.

Severity	Response Variables	Explanatory Variables	Mean Absolute Error (MAE)	Percent Variance Explained	mtry
all	magnitude	severity, elevation, and slope	21,949.49	46.88	3
high	magnitude	elevation, slope, and aspect	20,461.66	18.12	2
medium	magnitude	elevation, slope, and aspect	31,936.84	−6.03	2
low	magnitude	elevation, slope, and fire regime	2287.456	10.77	2
all	rate	severity, elevation, and slope	763.1918	33.13	2
high	rate	elevation, slope, and aspect	2536.23	23.45	2
medium	rate	elevation, slope, and aspect	819.4543	−9.18	2
low	rate	elevation, slope, and aspect	56.15127	−11.5	2

Note: We used mtry, the number of variables randomly sampled, as candidates at each split to parameterize.

## 4. Discussion

We analyzed spectral changes based on LandTrendr following three large (>16,000 ha), mixed-severity fires in lodgepole pine forests in the Southern Rocky Mountains. The NBR time series were compared with the data on post-fire climate, burn severity, topography, and geology to identify potential drivers of spectral recovery. We found LandTrendr to be an effective way of tracking spectral recovery over space and time. Our results indicated that the spectral recovery in the Southern Rocky Mountains was highly variable and influenced by fire severity and post-fire growing-season temperatures. In terms of both spectral recovery measurements presented here and field-based results [6], the climate (minimum growing-season temperature) and the topography (elevation, slope, and aspect) were the more important determinants in post-fire forest recovery.

Resilience was measured as the ability to return to a pre-fire spectral state. We analyzed the resilience in two ways, i.e., based on the annual NBR values and the annual %NBR recovery. The annual NBR values allowed us to compare the NBR values between fires and burn severity. When comparing the annual NBR values 15 years post-fire, there was no difference in the spectral reflectance between burn severities. Instead, the biggest difference in the NBR was between fire events, indicating that climate may be the primary driver of forest resilience.

The use of the annual %NBR recovery allowed us to compare how much the burned areas recovered in relation to their pre-fire spectral states. None of the burned areas returned to their pre-fire spectral values. However, stands burned at a high severity level recovered the most. From this perspective, resilience was most pronounced in patches that burned at a high severity level. This may be indicative of lodgepole pine's adaptation of serotinous cones that release seeds only after high-severity fires. As high-severity fires become larger, more frequent, and more severe in the decades ahead, serotinous lodgepole pine will likely have a competitive advantage over other conifer species that rely on seed dispersal [2]. However, if fires become too severe, seeds in serotinous cones can be damaged or consumed, and forest regeneration will become more dependent on the wind dispersal of seeds from surrounding stands [2]. Similarly, short intervals between stand-replacing fires may reduce the abundance of available seeds (which are not produced in abundance until maturity 15 years later), further increasing the reliance on wind-dispersed seeds [43,44]. Thus, if climate change significantly increases fire severity or frequency, then the resilience of lodgepole pine to high-severity fires may decrease from a reduced seedbank. Patches burned at a low severity level had the slowest rate and smallest magnitude of the annual post-fire NBR recovery. The slow recovery is most likely because low-severity fires have little effect on the stand structure, tree density, and crown surface area [45,46] and thus provide fewer opportunities for new establishment or growth compared to more severe fires. The use of the annual %NBR recovery as a metric of resilience showed how a stand spectrally recovers in relation to its pre-fire spectral state. However, the use of percentages predisposes the analysis to exaggerate the recovery following severe fires and minimizes the importance of forests remaining closer to their pre-fire states following low- and moderate-severity fires.

The biggest difference in forest recovery was among fire events, indicating that post-fire climate may be the most crucial variable in recovery capacity. Following the 2006 fire, stands that were burned at all severities recovered to similar pre-fire spectral states. In comparison, stands that were burned in the 1999 and 2002 fires did not recover to similar pre-fire spectral states, regardless of burn severity. The post-fire summer temperature following the 2006 fire was warmer than those following the 2002 and 1999 fires, suggesting a slightly warmer post-fire temperature may help initial post-fire recovery.

Although the data presented here point to climatic variability as a dominant factor in determining post-fire regeneration, we recognize that other factors could contribute to variation in regeneration among fires. These include biological factors, soil moisture, competitive interactions, and other variables that are not easily monitored with remote sensing.

The findings of the current study are consistent with field-based analysis, which found that post-fire recovery was limited by post-fire growing-season temperature [6,47]. In the future, a warming growing summer season may promote post-fire regeneration at some sites and inhibit regeneration at other sites [48]. For example, seedlings may be able to establish and survive at high elevations where historically cool conditions have limited the expansion of the upper treeline [48]. In contrast, warmer summer temperatures may continue to compromise post-fire recovery at lower elevations and warmer sites, as noted by the poor recovery following fires in 1999 and 2002. The present study indicates that, as warming continues, there may be changes in forest density where forests are not regenerating to their pre-fire spectral state. The combination of increasing climatically driven disturbances and unfavorable post-disturbance conditions could lead to increased forest patchiness or conversion to a non-forest state.

## 5. Conclusions

Landsat NBR SIs successfully documented changes in post-fire recovery in lodgepole pine forests following three high-severity fires. As climate change continues to increase wildfire activity, remote sensing information will continue to be valuable in documenting changes in forest density in the years after each event. We found that regeneration was most prolific following high-severity burns and at high elevations, but that regeneration was most strongly influenced by climate, such that the minimum and mean growing-season temperatures appear to limit post-fire recovery at lower elevations, which has implications for future forest dynamics and ecological trajectories. The combination of Landsat data and field observations is helpful in detecting and monitoring different aspects of post-disturbance resilience under climate change.

**Author Contributions:** Conceptualization, J.G, F.S. and D.K.; methodology, J.G, F.S. and D.K.; validation, J.G. and F.S.; formal analysis, J.G.; investigation, J.G.; resources, J.G.; data curation, J.G.; writing—original draft preparation, J.G.; writing—review and editing, J.G, F.S. and D.K.; visualization, J.G.; supervision, F.S. and D.K. All authors have read and agreed to the published version of the manuscript.

**Funding:** This research was funded by the Society of Women’s Geographers.

**Institutional Review Board Statement:** Not applicable.

**Informed Consent Statement:** Not applicable.

**Data Availability Statement:** The data and the code will be shared in Zenodo: <https://zenodo.org/badge/latestdoi/468425640>, accessed on 3 November 2021.

**Acknowledgments:** We would like to thank the anonymous reviewers.

**Conflicts of Interest:** The authors declare no conflict of interest.

## References

1. Higuera, P.E.; Shuman, B.N.; Wolf, K.D. Rocky Mountain subalpine forests now burning more than any time in recent millennia. *Proc. Natl. Acad. Sci. USA* **2021**, *118*, e2103135118. [[CrossRef](#)] [[PubMed](#)]
2. Guz, J.; Kulakowski, D. Forests in the Anthropocene. *Ann. Am. Assoc. Geogr.* **2020**, *111*, 869–879. [[CrossRef](#)]
3. Calder, W.J.; Shuman, B. Extensive wildfires, climate change, and an abrupt state change in subalpine ribbon forests, Colorado. *Ecology* **2017**, *98*, 2585–2600. [[CrossRef](#)] [[PubMed](#)]
4. Calder, W.J.; Parker, D.; Stopka, C.J.; Jiménez-Moreno, G.; Shuman, B.N. Medieval warming initiated exceptionally large wildfire outbreaks in the Rocky Mountains. *Proc. Natl. Acad. Sci. USA* **2015**, *112*, 13261–13266. [[CrossRef](#)] [[PubMed](#)]
5. Muir, P.S.; Lotan, J.E. Disturbance History and Serotiny of *Pinus contorta* in Western Montana. *Ecology* **1985**, *66*, 1658–1668. [[CrossRef](#)]
6. Guz, J.; Gill, N.S.; Kulakowski, D. Long-Term Empirical Evidence Shows Post-Disturbance Climate Controls Post-Fire Regeneration. *J. Ecol.* **2021**, *109*, 4007–4024. [[CrossRef](#)]
7. Stevens-Rumann, C.; Morgan, P. Repeated wildfires alter forest recovery of mixed-conifer ecosystems. *Ecol. Appl.* **2016**, *26*, 1842–1853. [[CrossRef](#)]
8. Harris, L.B.; Drury, S.A.; Taylor, A.H. Strong Legacy Effects of Prior Burn Severity on Forest Resilience to a High-Severity Fire. *Ecosystems* **2021**, *24*, 774–787. [[CrossRef](#)]
9. Chuvieco, E.; Aguado, I.; Salas, J.; García, M.; Yebra, M.; Oliva, P. Satellite Remote Sensing Contributions to Wildland Fire Science and Management. *Curr. For. Rep.* **2020**, *6*, 81–96. [[CrossRef](#)]
10. Hardy, C.C.; Burgan, R.E. Evaluation of NDVI for Monitoring Live Moisture in Three Vegetation Types of the Western US. *Photogramm. Eng. Remote Sens.* **1999**, *65*, 603–610.
11. Robinson, J.M. Fire from space: Global fire evaluation using infrared remote sensing. *Int. J. Remote Sens.* **1991**, *12*, 3–24. [[CrossRef](#)]
12. Anderegg, W.R.L.; Trugman, A.T.; Badgley, G.; Anderson, C.M.; Bartuska, A.; Ciais, P.; Cullenward, D.; Field, C.B.; Freeman, J.; Goetz, S.J.; et al. Climate-driven risks to the climate mitigation potential of forests. *Science* **2020**, *368*, eaaz7005. [[CrossRef](#)] [[PubMed](#)]
13. Rogers, B.M.; Balch, J.K.; Goetz, S.J.; Lehmann, C.E.R.; Turetsky, M. Focus on changing fire regimes: Interactions with climate, ecosystems, and society. *Environ. Res. Lett.* **2020**, *15*, 030201. [[CrossRef](#)]
14. Yuan, C.; Liu, Z.; Zhang, Y. Aerial Images-Based Forest Fire Detection for Firefighting Using Optical Remote Sensing Techniques and Unmanned Aerial Vehicles. *J. Intell. Robot. Syst.* **2017**, *88*, 635–654. [[CrossRef](#)]



15. Mueller, E.; Skowronski, N.; Clark, K.; Gallagher, M.; Kremens, R.; Thomas, J.C.; El Houssami, M.; Filkov, A.; Hadden, R.M.; Mell, W.; et al. Utilization of remote sensing techniques for the quantification of fire behavior in two pine stands. *Fire Saf. J.* **2017**, *91*, 845–854. [[CrossRef](#)]
16. Turner, M.G.; Hargrove, W.W.; Gardner, R.H.; Romme, W.H. Effects of Fire on Landscape Heterogeneity in Yellowstone National Park, Wyoming. *J. Veg. Sci.* **1994**, *5*, 731–742. [[CrossRef](#)]
17. McKenna, P.; Lechner, A.; Phinn, S.; Erskine, P. Remote Sensing of Mine Site Rehabilitation for Ecological Outcomes: A Global Systematic Review. *Remote Sens.* **2020**, *12*, 3535. [[CrossRef](#)]
18. Filipponi, F.; Manfron, G. Observing Post-Fire Vegetation Regeneration Dynamics Exploiting High-Resolution Sentinel-2 Data. *Proceedings* **2019**, *18*, 10. [[CrossRef](#)]
19. Roteta, E.; Bastarrika, A.; Padilla, M.; Storm, T.; Chuvieco, E. Development of a Sentinel-2 Burned Area Algorithm: Generation of a Small Fire Database for Sub-Saharan Africa. *Remote Sens. Environ.* **2019**, *222*, 1–17. [[CrossRef](#)]
20. Szpakowski, D.M.; Jensen, J.L.R. A Review of the Applications of Remote Sensing in Fire Ecology. *Remote Sens.* **2019**, *11*, 2638. [[CrossRef](#)]
21. Frazier, R.J.; Coops, N.C.; Wulder, M.; Hermosilla, T.; White, J. Analyzing spatial and temporal variability in short-term rates of post-fire vegetation return from Landsat time series. *Remote Sens. Environ.* **2018**, *205*, 32–45. [[CrossRef](#)]
22. Hislop, S.; Jones, S.; Soto-Berelov, M.; Skidmore, A.; Haywood, A.; Nguyen, T.H. Using Landsat Spectral Indices in Time-Series to Assess Wildfire Disturbance and Recovery. *Remote Sens.* **2018**, *10*, 460. [[CrossRef](#)]
23. Bright, B.C.; Hudak, A.T.; Kennedy, R.E.; Braaten, J.D.; Khalyani, A.H. Examining post-fire vegetation recovery with Landsat time series analysis in three western North American forest types. *Fire Ecol.* **2019**, *15*, 8. [[CrossRef](#)]
24. Lutes, D.C.; Keane, R.E.; Caratti, J.F.; Key, C.H.; Benson, N.C.; Sutherland, S.; Gangi, L.J. FIREMON: Fire effects monitoring and inventory system. *Gen. Tech. Rep.* **2006**, *164*, LA-1-55. [[CrossRef](#)]
25. Pleniou, M.; Koutsias, N. Sensitivity of spectral reflectance values to different burn and vegetation ratios: A multi-scale approach applied in a fire affected area. *ISPRS J. Photogramm. Remote Sens.* **2013**, *79*, 199–210. [[CrossRef](#)]
26. Eidenshink, J.; Schwind, B.; Brewer, K.; Zhu, Z.-L.; Quayle, B.; Howard, S. A Project for Monitoring Trends in Burn Severity. *Fire Ecol.* **2007**, *3*, 3–21. [[CrossRef](#)]
27. Chu, T.; Guo, X. Remote Sensing Techniques in Monitoring Post-Fire Effects and Patterns of Forest Recovery in Boreal Forest Regions: A Review. *Remote Sens.* **2014**, *6*, 470–520. [[CrossRef](#)]
28. Idris, M.H.; Kuraji, K.; Suzuki, M. Evaluating Vegetation Recovery Following Large-Scale Forest Fires in Borneo and North-eastern China Using Multi-Temporal NOAA/AVHRR Images. *J. For. Res.* **2005**, *10*, 101–111. [[CrossRef](#)]
29. Pickell, P.D.; Hermosilla, T.; Frazier, R.J.; Coops, N.; Wulder, M. Forest recovery trends derived from Landsat time series for North American boreal forests. *Int. J. Remote Sens.* **2015**, *37*, 138–149. [[CrossRef](#)]
30. Zhao, B.; Zhong, Y.; Zhang, L. A spectral-structural bag-of-features scene classifier for very high spatial resolution remote sensing imagery. *ISPRS J. Photogramm. Remote Sens.* **2016**, *116*, 73–85. [[CrossRef](#)]
31. Amiro, B.D.; Barr, A.; Black, T.A.; Bracho, R.; Brown, M.; Chen, J.; Clark, K.L.; Davis, K.J.; Desai, A.; Dore, S.; et al. Ecosystem carbon dioxide fluxes after disturbance in forests of North America. *J. Geophys. Res. Earth Surf.* **2010**, *115*. [[CrossRef](#)]
32. Holling, C.S. Resilience and Stability of Ecological Systems. *Annu. Rev. Ecol. Syst.* **1973**, *4*, 1–23. [[CrossRef](#)]
33. Gunderson, L.H. Ecological Resilience—In Theory and Application. *Annu. Rev. Ecol. Syst.* **2000**, *31*, 425–439. [[CrossRef](#)]
34. Chu, T.; Guo, X.; Takeda, K. Effects of Burn Severity and Environmental Conditions on Post-Fire Regeneration in Siberian Larch Forest. *Forests* **2017**, *8*, 76. [[CrossRef](#)]
35. Chambers, M.E.; Fornwalt, P.J.; Malone, S.L.; Battaglia, M.A. Patterns of conifer regeneration following high severity wildfire in ponderosa pine—Dominated forests of the Colorado Front Range. *For. Ecol. Manag.* **2016**, *378*, 57–67. [[CrossRef](#)]
36. Haffey, C.; Sisk, T.D.; Allen, C.D.; Thode, A.E.; Margolis, E.Q. Limits to Ponderosa Pine Regeneration following Large High-Severity Forest Fires in the United States Southwest. *Fire Ecol.* **2018**, *14*, 143–163. [[CrossRef](#)]
37. Turner, M.G.; Turner, D.M.; Romme, W.H.; Tinker, D.B. Cone production in young post-fire *Pinus contorta* stands in Greater Yellowstone (USA). *For. Ecol. Manag.* **2007**, *242*, 119–126. [[CrossRef](#)]
38. Team, R.C. *R: A Language and Environment for Statistical Computing*; R Core Team: Vienna, Austria, 2013.
39. Fox, J.; Weisberg, S. Multivariate Linear Models in R. In *An R Companion to Applied Regression*; Sage Publications: London, UK, 2011.
40. Breiman, L. Bagging Predictors. *Mach. Learn.* **1996**, *24*, 123–140. [[CrossRef](#)]
41. Liaw, A.; Wiener, M. Classification and Regression by randomForest. *R News* **2002**, *2*, 18–22.
42. Rother, M.T.; Veblen, T.T. Limited conifer regeneration following wildfires in dry ponderosa pine forests of the Colorado Front Range. *Ecosphere* **2016**, *7*. [[CrossRef](#)]
43. Hansen, W.D.; Brazionas, K.H.; Rammer, W.; Seidl, R.; Turner, M.G. It takes a few to tango: Changing climate and fire regimes can cause regeneration failure of two subalpine conifers. *Ecology* **2018**, *99*, 966–977. [[CrossRef](#)] [[PubMed](#)]
44. Lotan, J.E. Cone Serotiny-Fire Relationships in Lodgepole Pine. *Bark Beetles Fuels Fire Bibliogr.* **1976**, *8*, 267–278.
45. Sibold, J.S.; Veblen, T.T. Relationships of Subalpine Forest Fires in the Colorado Front Range with Interannual and Multidecadal-Scale Climatic Variation. *J. Biogeogr.* **2006**, *33*, 833–842. [[CrossRef](#)]
46. Schumacher, S.; Bugmann, H. The relative importance of climatic effects, wildfires and management for future forest landscape dynamics in the Swiss Alps. *Glob. Chang. Biol.* **2006**, *12*, 1435–1450. [[CrossRef](#)]

47. Harvey, B.J.; Donato, D.C.; Turner, M.G. High and Dry: Postfire Drought and Large Stand-Replacing Burn Patches Reduce Postfire Tree Regeneration in Subalpine Forests. In *Causes and Consequences of Spatial Patterns of Fire Severity in Northern Rocky Mountain Forests: The Role of Disturbance Interactions and Changing Climate*; The University of Wisconsin-Madison: Madison, WI, USA, 2016; Volume 1001, p. 224.
48. Davis, K.T.; Dobrowski, S.Z.; Higuera, P.E.; Holden, Z.A.; Veblen, T.T.; Rother, M.T.; Parks, S.A.; Sala, A.; Maneta, M.P. Wildfires and climate change push low-elevation forests across a critical climate threshold for tree regeneration. *Proc. Natl. Acad. Sci. USA* **2019**, *116*, 6193–6198. [[CrossRef](#)] [[PubMed](#)]